Autofocusing-based visual servoing : application to MEMS micromanipulation.

Guillaume Duceux, Brahim Tamadazte, Nadine Le Fort - Piat, Eric Marchand, Guillaume Fortier, Sounkalo Dembélé

Autofocusing-based visual servoing: application to MEMS micromanipulation

G. Duceux, B. Tamadazte, N. Le-Fort Piat, E. Marchand, G. Fortier, and S. Dembélé

Abstract— **In MEMS microassembly areas, different methods of automatic focusing are presented in the literature. All these methods have a common point. Thus, the current autofocusing methods for microscopes need to perform a scanning on all the vertical axis of the microscope in order to find the peak corresponding to the focus (sharpen image). Those methods are time consuming. Therefore, this paper presents an original method of autofocusing based on a velocity control approach which is developed and validated on real experiments.**

I. Overview

Reliable autofocusing methods are indispensable in the microassembly of hybrid micro-electromechanical systems (MEMS) and for general uses of optical microscopes [6], [8]. Ensuring an optimal focus is essential in industrial vision systems. A good focus ensures sharpen image and thus improves the reliability of vision algorithms. Meanwhile, the availability of high resolution cameras and powerful microprocessors have made possible for vision systems to play a key role in the automatic microsystems assembly area.

Implementing an autofocus for an optical microscope solves different difficulties. Firstly, the depth-of-field is weak in optical microscopy. Therefore, visual features extraction is not effective on blurred image. Another consequence is that image quality is more sensitive to lighting, exposure time and noise perturbations. Thus, reliability is more difficult to obtain with optical microscopes.

Traditional autofocus methods are based on a cost function which presents a maximum corresponding to the position of the optical microscope given the sharpest image. To obtain this sharpest image, autofocus methods proceed with a vertical scanning on the microscope focus range. The microscope moves to different positions with a fixed step, and for each position the cost function is computed. Considering that depth of field is very weak, to ensure usable images, the scanning step has to be really small with regards to common vision system. Therefore, those kind of methods are time consuming. If the object has a vertical movement, to keep the focus on it, move presicely the microscope, or do the autofocus once again on a smaller range. Actually, for each application, a good autofocus method has to be found by choosing the range, the step and the cost function with regards to the situation.

G. Duceux, B. Tamadazte, N. Le Fort-Piat, and S. Dembélé are with FEMTO-ST Institute-AS2M/UMR CNRS 6174 /UFC/ EN-SMM / UTBM, 24 rue Alain Savary, 25000 Besançon, France, brahim.tamadazte@ens2m.fr

E. Marchand is with Université de Rennes 1, IRISA, INRIA Rennes-Bretagne Atlantique, Lagadic

G. Fortier is with INRIA Rennes-Bretagne Atlantique, IRISA, Lagadic, France

To provide a dynamic, fast and accurate autofocus, more elaborated methods have to be found. This paper presents an original method in which the focus is found by controlling the velocity of the microscope with an adaptive gain. The main purpose of this research is to perform faster autofocus by investigating different approaches (cost functions).

The paper is structured as follow: Section II presents the equipments and the configuration used for this study. Section III details the modelling which concerns visual servoing, traditional autofocus and the developed focus-based visual servoing. Section IV presents experimental results.

II. Experimental setup

The proposed autofocus method was experimented on a MEMS microassembly station (Fig. 1). The goal is to find the focus on the positioning platform or on the gripper. The experimental set-up used to validate the concepts developed, includes a robotic system in combination with a gripping system and an imaging system. The whole set-up is positioned on a vibration-free table inside a controlled environment as required by this kind of experiment (Fig. 1).

A PC is connected by a serial link, to the microscope (Fig. 2). It processes the information and computes the algorithm. It is a Intel Core 2 Duo, CPU 3.16 GHz, 3.25 Go of RAM.

The imaging system includes a microscope positioned vertically. It is a LEICA MZ 16 A optical video stereomicroscope. The zoom (and then the magnification) and the focus are motorized and controlled by the PC. The magnification ranges from $\times 0.71$ to $\times 11.5$. The field-of-view varies from 700 μm $\times$ 900 μm with a resolution of 1.4 μm at the maximum of the magnification ($\times 11.5$) to 20 mm $\times$ 25 mm with a resolution of 21 mm at the minimum of magnification ($\times 0.71$). The depth-of-field varies from 2.9 mm to 0.035 mm according to the numerical aperture of the objective. The work distance is approximately 112 mm.

Most of experiments results were performed with a frame rate of 12 fps. To send a request to the motors, via the serial link takes approximately 20 milliseconds. The whole algorithm has a treatment rate of 7 frames per second.

III. Focus-based visual servoing

As already stated, the objective is to find the focus position automatically and quickly in order to ensure good condition for industrial vision algorithms in automated processes. This task is known as autofocus. To perform that, different cost functions which ususally reflects the sharpness of the image contour were implemented and evaluated. With respect to

!htbp

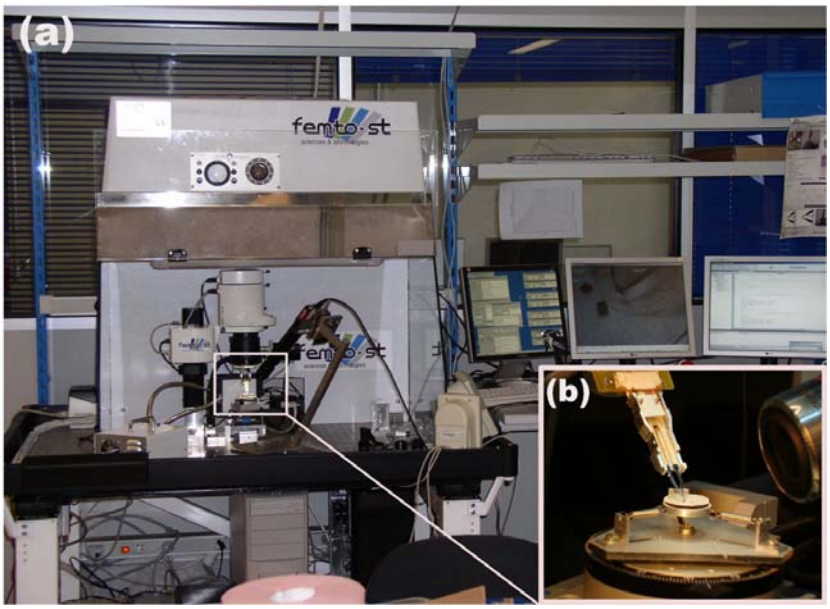

Fig. 1. (a) Global view of the microassembly workcell and (b) shows a zooming on the positioning platform.

Fig. 2. The MZ16A optical microscope from Leica Instruments used in the experimental setup.

classical autofocus approaches where an exhaustive scan is usually performed, following visual servoing approaches, we proposed a gradient-based method that allows a continuous autofocus.

A. Common autofocus approaches

Autofocus is a kind of visual servoing task that is generally performed in first. The autofocus task consists on finding the position on the optical axis of an optical microscope (or camera) that provides the more usable or sharpen images. Classical approaches are based on the maximization of a cost function C. The common approach consists in scanning a range of positions $\mathbf{r}$ with a fixed step. For each position, the cost is computed with the current image. At the end of the scan, the focus position should be the one corresponding to a peak of the cost function. A comparison of cost functions was described in [9], [2], [4]. More details on common autofocusing methods are presented in [3] and [5].

These traditional autofocus have a set of well known issues: they are slow, a good cost function has to be find for each situation, and a lot of parameters have to be adjusted to perform a good automated process in term of rate, precision and adaptability.

B. Autofocus cost functions

Many focusing algorithms have been proposed and compared in [9], [2], [4]. For traditional focusing algorithms, the output (cost function) of an ideal focus algorithm is defined as having a maximum value at the best focused image/position. In [9], the focus algorithms used in the literature are compared and tested in detail. In the context of our study, different cost functions were selected and used in the proposed autofocus-based visual control.

- **Derivative-based algorithms**
  - ***Gradient***:

$$C_{gradient} = \sum_{H}\sum_{W} \nabla I_x(i,j) + \nabla I_y(i,j) \qquad (1)$$

    where I represents the gray level intensity of the pixel at the coordinate (i,j). H and W are the Height and the Width of the image.
  - ***Laplacian***:

$$C_{Laplacian} = \sum_{H}\sum_{W} \Delta I(i,j) \qquad (2)$$

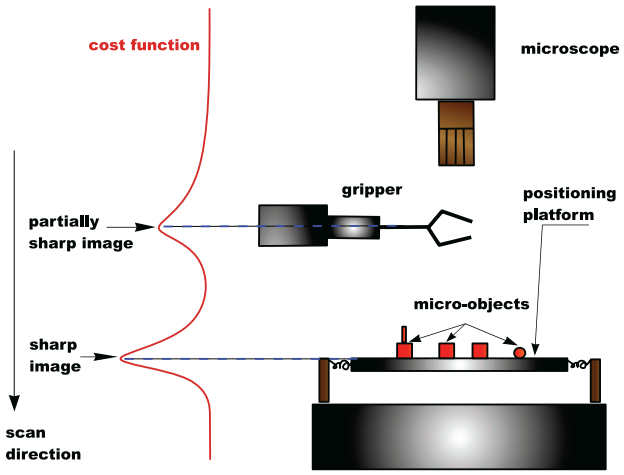

Fig. 3. Principe of the autofocus achievement.

using the following mask:

$$\Delta I(i,j) = \begin{pmatrix} -1 & -4 & -1 \\ -4 & 20 & -4 \\ -1 & -4 & -1 \end{pmatrix} \quad (3)$$

- **Statistics-based algorithms**
  - ***Variance***:

$$C_{variance} = \frac{1}{H.W} \sum_H \sum_W (I(i,j) - \mu)^2 \quad (4)$$

with:

$$\mu = \frac{1}{H.W} \sum_H \sum_W I(i,j) \quad (5)$$

  - ***Normalized variance***: this technique allows the normalization of the final output with the mean intensity μ.

$$C_{nvariance} = \frac{1}{H.W.\mu} \sum_H \sum_W (I(i,j) - \mu)^2 \quad (6)$$

  - ***Autocorrelation***:

$$C_{auto-corr} = \sum_H \sum_W I(i,j) \cdot I(i+1,j) - H \cdot W \cdot \mu^2 \quad (7)$$

- **Histogram-based algorithms**
  These algorithms use histogram $h(i)$: the number of pixels with intensity i in the image.
  - ***Range algorithm***: this algorithm computes the difference between the highest and the lowest intensity levels.

$$C_{range} = max_{(0 \le i \le 255)}(h(i) > 0) - min_{(0 \le i \le 255)}(h(i) > 0) \quad (8)$$

  - ***Entropy algorithm***: it assumes that focused images contain more information than blurred images.

$$C_{entropy} = - \sum_{0 \le i \le 255} p_i \cdot log_2(p_i) \quad (9)$$

where $p_i = h(i)/H \cdot W$ is the probability of a pixel with intensity i.

- **Other algorithms**
  - ***Image power***:

$$C_{power} = \sum_H \sum_W I(i,j)^2 \quad (10)$$

This algorithm sums the square of image intensities of each pixel i.

The normalized variance (see equation (6)) is the cost function that has been selected for our study. It presented the better behavior and stability to condition changes. Whatever the parameters applied on the microscope, the noise is still significant on the cost function, a low pass filter can be applied on the function with usually good results. Unfortunately, that increases the computational time, which is critic in velocity-controlled algorithm.

C. Visual servoing

Visual servoing is a well known technique in robot control that allows to achieve robotic tasks from visual features acquired by a camera. In common approach, the control law is designed to move a robot so that the current visual features $\mathbf{s}$, acquired from the current pose $\mathbf{r}$, will reach the desired features $\mathbf{s}^*$ acquired at the desired pose $\mathbf{r}^*$ [1]. The control law is thus designed to vanish the error given by:

$$\mathbf{e} = \mathbf{s} - \mathbf{s}^* \quad (11)$$

To build the control law, the knowledge of the interaction matrix $\mathbf{L_s}$ that links the feature variation to the camera velocity $\dot{\mathbf{s}} = \mathbf{L_s}\mathbf{v}$ is usually required. The camera velocity is then given by $\mathbf{v} = -\lambda \mathbf{L_s^+}\mathbf{e}$.

With respect to classical visual servoing techniques, the proposed approach presents two main differences:

- first, here our goal is not to minimize an error $\mathbf{e}$ but to maximize the cost function given by equation (6).
- second, considering equation (6) it is not necessary as for classical visual servoing approaches to extract features $\mathbf{s}$ (points, lines, pose, etc.) from the image. Rather, we will consider the image as a whole and consider all its pixels.

We built a control law that directly control the velocity of the optical microscope. The control law is composed of the gradient and a gain. The gradient of the cost function gives the direction in which the microscope should move. It is written as following:

$$\mathbf{v} = \lambda(C,h,k).\frac{\nabla C}{\|\nabla C\|} \quad (12)$$

where ∇C is the gradient of the cost function given by equation (6) wrt. the microscope velocity along its optical axes. Let I_n denote the image taken at the discrete time n, then ∇C is given by:

$$\nabla C = C(I_n) - C(I_{n-1}) \quad (13)$$

where

Different gains had been tested. From these gains we have selected the following which presented the best behavior of

the control law (i.e. convergence and stability). It is given by:

$$\left| \begin{array}{lll} \lambda(C,h,k) = & h\left(\frac{C_0}{C}\right)^k & if \quad \frac{C_0}{C} < 1 \\ \lambda(C,h,k) = & h & else \end{array} \right. \tag{14}$$

where h and k are two positive integers, and C_0 is the cost function computed at the initial position.

The adaptive gain $\lambda(C)$ is an important part and it has to be adjusted. The first condition is that far from the focus position, the velocity should be big enough to avoid small perturbations and thus oscillations. This is the role of h. It represents the maximum velocity. The second condition is that near the focus position, the velocity is zero. k is there for that purpose. Indeed, if $(\frac{C_0}{C})$ does not decrease enough near the focus position, the velocity will be too high to focus precisely. Finally, C_0 is the evaluation of the cost function corresponding to the initial image/position.

Different solutions have been developed and tested to stop the proposed autofocus technique when the sharpen image is found. The selected solution is the following: a well adjusted autofocus-based visual servoing algorithm should only oscillate around the focus, so the algorithm can be stopped when the gradient direction changes.

D. Discussion

The autofocus presented in this paper is made to do a static autofocus. But it may be used to perform a dynamic one, meaning that it is possible to track an object (for example the gripper) on its vertical displacement during the different micromanipulation and microassembly tasks. In fact, in microassembly, research intend to assemble MEMS in complex ways. In order to do this, as the depth-of-field is narrow, the focus has to be adjusted to put a MEMS on the top of another one.

IV. Experimental results

The purpose of this work was to find a quicker autofocus, and explore a new approach. Experimental validations have been made of course in order to validate this approach, but also to compare this method with traditional ones.

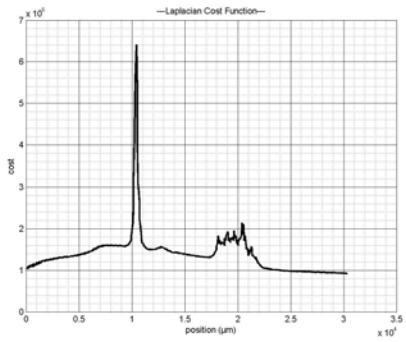

Fig. 4. Cost function of the Laplacian with good conditions.

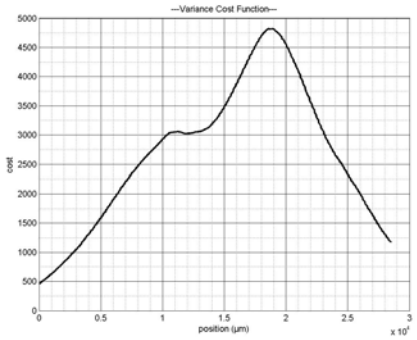

Fig. 5. Cost function of the variance with good conditions.

Figure 4 and figure 5 illustrate the cost function obtained using the variance and Laplacian methods, respectively. These curves are obtained in perfect conditions of illumination. This explains the smoothness of the curves (lack of transitions caused by the lighting fluctuations). The maximum of each curve represents the relative position of the sharpness image from the start position of the optical microscope before the vertical scanning.

These methods are reproduced with perturbations (i.e. changing light). So, figure 6 and 7 show the same cost functions curves (i.e. Laplacian and variance approaches), respectively. In this case, the behaviors of these techniques change and cause small and repetitive transitions in the curves. Despite these inconvenient behaviors of the cost functions due to unstable lighting, it has been demonstrated that the proposed autofocus-based visual servoing remains effective and precise.

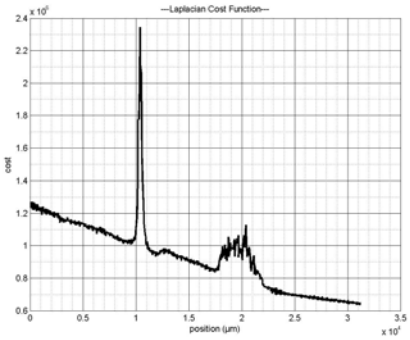

Fig. 6. Cost function of the Laplacian with perturbations.

Another approach presents a good behavior of its cost function, this is true in both cases: good conditions or unstable lighting. Where a pass low filter is added to the normalized variance, it can be seen that the maximum of the cost function curve is well represented (see, Fig. 8).

It can be noticed in the previous studied examples that the cost functions and autofocus methods are sensitive to many factors: lighting, magnification, exposure time, as explained in [7]. However, the developed autofocus-based visual ser-

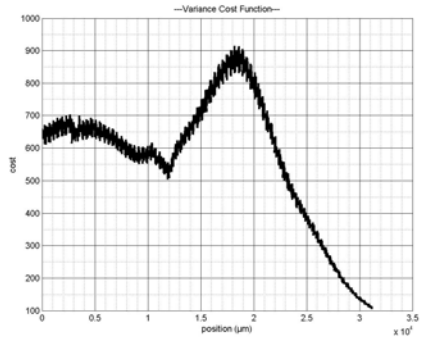

Fig. 7. Cost function of the variance with perturbations.

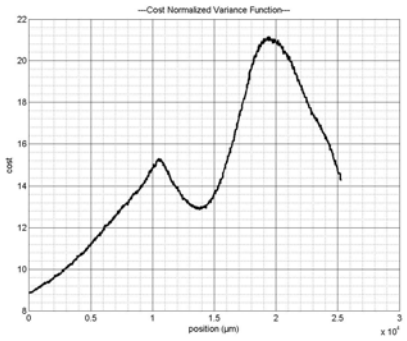

Fig. 8. Cost function of the normalized variance with a low pass filter.

voing presents some advantages despite these perturbations. From the both studied approaches (traditional and proposed techniques), it can be noticed that the proposed approach remains more robust against the perturbations and more precise. Among the methods used, the normalized variance (Fig. 8) is the technique which presents the best compromise speed/robustness. Moreover, the fact to normalize the cost function values during the acquisition allows to reduce the perturbations effects. This is even more interesting when a low pass filter is added to the cost function. This filter is given by the following relationship:

$$C_f = 0.5 * C_k + 0.5 * C_{k-1} \tag{15}$$

Nevertheless, as it can be seen with comparison between traditional autofocus and autofocus-based visual servoing, it brings some serious advantages. This is more interesting when the control law is done with an adaptive gain. The idea is to use a large proportional gain to accelerate the scanning of the microscope initially, when it is far from the sharpness image (i.e. in the first part of cost function curve). Once it begins to approach the maximum value of the cost function, the microscope velocity should exponentially decrease. Therefore, the adaptive gain λ_a can be adjusted in order to decrease this velocity. Over, the use of this type of adaptive control law allows to avoid the local maximum of the cost function curves. The gain λ_a is function of the gradient of the curve and is given by:

$$\left| \begin{array}{c} \lambda_a = h.\left(\frac{C_0}{C}\right)^k \quad if \quad \frac{C_0}{C} < 1 \\ \lambda_a = h \quad else \end{array} \right. \tag{16}$$

where h and k are positive integers. The experimental results presented in this paper are obtained with h = 1000 and k = 2. The behavior of λ_a obtained with such parameters is represented in Fig 9.

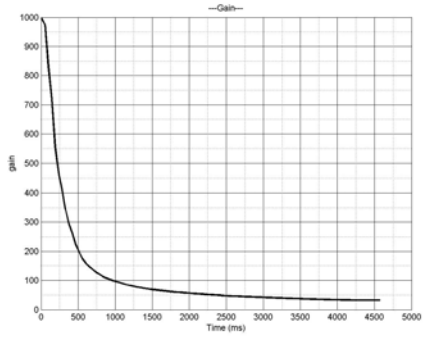

Fig. 9. Decreasing of the adaptive gain versus the number of iterations.

Concerning the time needed to find the sharpness image, a comparison test has been made between the traditional autofocus approaches and the proposed method. For instance, the traditional autofocus was performed with a scanning on the full range of positions and with a step of 100 μm. It found the focus positions in approximately 2 minutes. In the same conditions, the velocity-based autofocus was found the sharpen image in only 0.5 seconds (15 images are needed to perform the autofocusing process). The precision of the position of the sharpen image performed with the traditional technique is 119 μm while the precision estimated by the proposed method is 100 μm.

The comparison has been carried on with different initial conditions: restricted range, different steps, initial positions, and initial velocities and whatever was possible. The result is that the velocity-based autofocus was more faster despite the technology limitation which concern the limited communication speed between the computer and the optical microscope motorization.

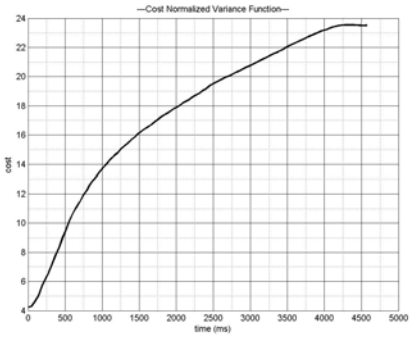

Fig. 10. Representation of the cost function.

Figure 10 illustrates the cost function-based normalized variance acquired during the achievement of the velocity-based autofocusing. It can be noticed that the optical microscope displacement is stopped precisely at the first maximum which represents the sharpen image vertical position. The corresponding velocity behavior sent to the focus motorization of the microscope is represented in the Fig. 11. Through the adjustable positive gain integrated to the control law, the decreasing of the velocity is exponential. However, a small oscillation appears a the end of the velocity curve, this is a test to ensuring that the maximum value of the cost function curve is well reached.

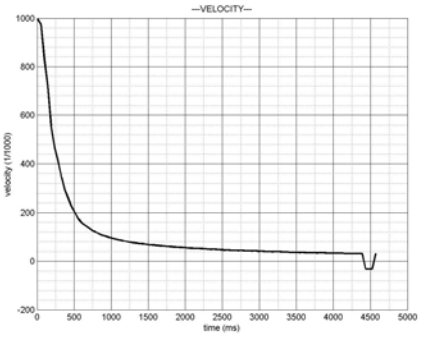

Fig. 11. Velocity versus number of iterations.

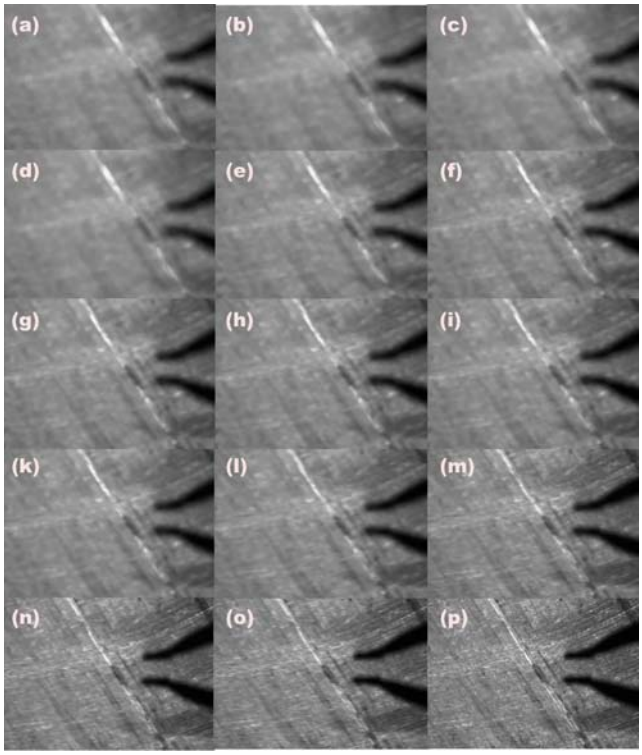

Fig. 12. shots captured during the autofocus process. Image (a) illustrates the initial position of the microscope (defocused position), image (b) to image (o) show the different images captured during the autofocusing process and image (p) represents the end of the focus-based visual servoing control (sharp image).

Figure 12 shows shots captured during the autofocus process. It took around 0.5 seconds to find the focus with a precision of 100 μm. This autofocus is performed with the presence of the microgripper in the vertical scan interval which adds difficulties to find the perfect sharpen image.

V. Conclusion and future perspectives

This paper has presented a new approach for autofocusing in order to make it faster and accurate. The method is based on the maximization of a cost function like common autofocus. But instead of proceeding with a scanning on image/position, the proposed approach is based on the control of the focus motorization velocity. Experimental results had shown that this method allows to perform fast autofocusing in general. Once adjusted to a specific microscope-based system, it allows to accelerate considerably the micromanipulation and microassembly processes.

The future work will be oriented on the use of these approaches: i.e. vision feedback control based on the use of the global image information (intensity, gradient, Laplacian) to automate MEMS micromanipulation and microassembly processes.

Aknowledgements

This work is partially conducted with financial support from the project Hybrid Ultra Precision Manufacturing Process Based on Positional and Self assembly for Complex Micro-Products (HYDROMEL NMP2-CT-2006-026622) funded by the European Commission.

The authors would like to thank David Guibert, from the FEMTO-ST Institute/AS2M department for his help in the development of the microscope support.

References

[1] B. Espiau, F. Chaumette, and P. Rives, *A new approach to visual servoing in robotics*, **8** (1992), no. 3, 313–326.

[2] G. Lightart F. Groen, I.T. Young, *A comparison of different focus functions for use in autofocus algorithms*, Cytometry **12** (1985), p.81–91.

[3] E. Krotkov, *Focusing*, International Journal of Computer Vision **1** (1987), p. 223–237.

[4] K. Culp N. Talsania K. Preston L. Firestone, K. Cook, *Comparison of autofocus methods for automated microscopy*, Cytometry **12** (1991), p.195–206.

[5] A. Nikzad M. Subbarao, T.S. Choi, *Focusing techniques*, Journal of Optical Engineering **32** (1993), p. 2824–2836.

[6] B. Tamadazte, N. Le-Fort Piat, E. Marchand, and S. Dembélé, *Microassembly of complex and solid 3d mems by 3d vision-based control*, IEEE Int. Conf. on Intelligent Robots and Systems, IROS'09 (St Louis, USA), October 2009, pp. 3284–3289.

[7] D. Vollath, *The influence of the scene parameters and of noise on the behavior of automatic focusing algorithm*, Journal of Microscopy **151** (1988), p. 133–146.

[8] G. Yang, J. Gaines, and B. Nelson, *A supervisory wafer-level 3d microassembly system for hybrid mems fabrication*, Journal of Intelligent and Robotic Systems **37** (2003), 43–68.

[9] Stefan Duthaler Yu Sun and Bradley J. Nelson, *Autofocusing algorithm selection in computer microscopy*, IEEE/RSJ International Conference on Intelligent Robots and Systems (2005), p. 419–425.